Molecular Determinants of Sugar Transport Regulation by ATP†

Kara B. Levine, Erin K. Cloherty, Stephanie Hamill, and Anthony Carruthers*

Department of Biochemistry and Molecular Pharmacology, Lazare Research Building, University of Massachusetts Medical School, 364 Plantation Street, Worcester, Massachusetts 01605

Received March 29, 2002; Revised Manuscript Received July 11, 2002

ABSTRACT: Intracellular ATP inhibits human erythrocyte net sugar transport by binding cooperatively to the glucose transport protein (GluT1). ATP binding produces altered transporter affinity for substrate and promotes substrate occlusion within a post-translocation vestibule formed by GluT1 cytosolic domains. The accompanying paper (Cloherty, E. K., Levine, K. B., Graybill, C., and Carruthers, A. (2002) *Biochemistry 41,* 12639−12651) demonstrates that reduced intracellular pH promotes high-affinity ATP binding to GluT1 but inhibits ATP-modulation of GluT1-mediated sugar transport. The present study explores the role of GluT1 residues 326−343 (a proposed GluT1 ATP-binding site subdomain) in GluT1 ATP binding by using alanine scanning mutagenesis. Cos-7 and HEK cells were transfected with a cDNA encoding full-length human GluT1 terminating in a carboxyl-terminal hemagglutinin (HA)-His_6 epitope. The transporter (GluT1.HA.H_6) is expressed at the surface of both cell-types and is catalytically active. In HEK cells, both parental GluT1- and GluT1.HA.H_6-mediated sugar transport are acutely sensitive to cellular metabolic inhibition. Isolated, detergent-solubilized GluT1.HA.H_6 is photolabeled by [γ-^{32}P]-azidoATP in an ATP-protectable manner. Alanine substitution of E_{329} or $G_{332}/R_{333}/R_{334}$ enhances GluT1.HA.H_6 [γ-^{32}P]azidoATP photoincorporation but blocks acute modulation of net sugar transport by cellular metabolic inhibition. These actions resemble those of reduced pH on ATP binding to and modulation of red cell GluT1. It is proposed that cooperative nucleotide binding to GluT1 and nucleotide modulation of GluT1-mediated sugar transport are regulated by a proton-sensitive saltbridge ($Glu_{329}-Arg_{333/334}$).

Human red blood cell sugar transport is mediated by the integral membrane protein GluT1[1] (*1*−*3*). Net sugar transport in human red blood cells is inhibited by intracellular ATP (*4*). ATP interacts allosterically with GluT1 to alter the tertiary structure of the GluT1 carboxyl terminus (*5*) and to promote substrate occlusion within a post-translocation pathway vestibule formed by GluT1 cytoplasmic domains (*6*). Non-hydrolyzable ATP analogues can substitute for ATP in GluT1 regulation, but intracellular AMP and ADP are unable to directly modulate transport. Rather, these nucleotides compete with ATP for binding to the glucose transporter and thereby competitively inhibit ATP-dependent sugar transport inhibition (5, *7*). When exposed to extracellular reductant, the red cell hexose transfer complex (a GluT1 tetramer) collapses to dimeric GluT1 (*8*), the cytosolic substrate occlusion vestibule opens (*6*), GluT1 ATP binding is severely diminished (*9*, *10*), and GluT1-mediated sugar transport is depressed and becomes unresponsive to intracellular ATP (*6*, *8*, *11*).

Reduced intracellular pH enhances ATP binding to red cell GluT1 but, paradoxically, blocks modulation of sugar transport by physiologic intracellular ATP levels (*9*, *10*). ATP binding to GluT1 is a positively cooperative process, and reduced pH converts the low affinity, unliganded carrier into a high-affinity ATP-binding complex (*10*). We have proposed that the GluT1 cytosolic substrate occlusion vestibule opens when all 4 GluT1 subunits of the sugar transporter complex are liganded by ATP at low pH (*10*). Sensitivity to H^+ over the concentration range 10 nM−10 μM suggests that GluT1 histidine side-chain protonation plays a role in modulating sensitivity to and/or binding of ATP. GluT1 contains 5 histidine residues of which four (H 160, 239, 337, and 484) are located within cytoplasmic domains. Exofacial His_{50} is an unlikely candidate since red cell sugar transport is insensitive to altered extracellular pH (*12*).

Human erythrocyte GluT1 contains three domains that share homology with human adenylate kinase nucleotide binding domains (*5*, *13*). The GluT1 signature Walker A motif (residues 111−117) lies in an exofacial GluT1 domain (*3*, *14*) and cannot be directly involved in nucleotide binding because ATP acts at an intracellular site on the glucose transporter (*9*). Adenylate kinase homology domain 2 (residues 225−229) lies in the central cytoplasmic loop of GluT1, and adenylate kinase homology domain 3 (AKHD3; GluT1 residues 332−343) is presented on GluT1 putative

† This work was supported by NIH Grant DK 36081.

* To whom correspondence should be addressed. Voice: 508 856 5570. FAX: 508 856 6464. E-mail:anthony.carruthers@umassmed.edu.

[1] Abbreviations: GluT1, human erythrocyte glucose transport protein; 2DOG, 2-deoxy-D-glucose; 3MG, 3-*O*-methyl-α,D-glucopyranoside; C-Ab, rabbit polyclonal antiserum raised against a synthetic peptide comprised of GluT1 residues 480−492; CCB, cytochalasin B; CCD, cytochalasin D; ∂-Ab, sheep polyclonal antiserum raised against native, nonreduced GluT1; EDTA, ethylenediaminetetraacetic acid; FCCP, carbonylcyanide-*p*-trifluoromethoxyphenyhydrazone; HA-Ab, mouse monoclonal antibody directed against the hemagglutinin sequence LYPYNVPNYA; HEPES, (N-[2-hydroxyethyl]piperazine-N′-[2-ethanesulfonic acid]); Ni−NTA, nickel−nitrilotriacetic acid; RBC, red blood cell; SDS-PAGE, sodium dodecyl sulfate-polyacrylamide gel electrophoresis; Tris−HCl, tris(hydroxymethyl)aminomethane.

10.1021/bi0258997 CCC: $22.00
Published on Web 09/26/2002

intracellular loop 5. AKHD 3 forms a hydrophobic pocket that flanks the adenine ribose and triphosphate chain of liganded Mg.ATP in adenylate kinase (*15*). Both AKHD2 and 3 contain or are in close proximity to H^+-sensitive histidine residues. Sequence analysis of peptides released upon proteolysis of azido ATP-photolabeled GluT1 indicates that GluT1 residues 301 through 364 form an integral component of the GluT1 ATP binding domain (*9*). GluT1 residues 307−327 and 338−358 are strongly hydrophobic, are predicted to form membrane-spanning domains (*3*) and are, therefore, unlikely to be accessible to cytosolic ATP. AKHD 3 is positioned in the intervening (cytosolic) sequence between these membrane-spanning regions and is a stronger candidate for direct interaction with ATP. The present study evaluates the role(s) of specific amino acids within GluT1 AKHD3 in nucleotide binding to GluT1.

MATERIALS AND METHODS

Materials. 8-Azido[γ^{32}P]ATP was purchased from ICN, Costa Mesa, CA. [^{3}H]-2-Deoxy-D-glucose was purchased from Dupont NEN, Wilmington, DE. Nitrocellulose and Immobilon-P were obtained from Fisher Scientific, Pittsburgh, PA. Dulbecco's Modified Eagle Medium, FBS, Penicillin/Streptomycin, and G418 (Geneticin) were purchased from Gibco BRL, Grand Island, NY. The QuickChange Site-Directed Mutagenesis Kit was acquired from Stratagene, Marco Island, FL. pcDNA3.1+ vector was supplied by Invitrogen, Carlsbad, CA. Fugene 6 Transfection Reagent, anti-HA antibody (mouse monoclonal HA-Ab), Endoproteinase Lys-C, and *N*-dodecyl-β-D-maltoside were obtained from Roche, Indianapolis, IN. Nickel−NTA column packing (Ni−NTA) was purchased from Qiagen, Valencia, CA. Centricon concentrators were acquired from Millipore, Bedford, MA. All remaining materials were purchased from Sigma unless stated otherwise.

Antisera. A peptide corresponding to GLUT1 residues 480−492 was synthesized by the University of Massachusetts Medical School Peptide Synthesis facility. This peptide was conjugated to keyhole limpet hemocyanin using a kit purchased from Pierce. Rabbit antisera (C-Ab) against this GluT1 peptide were obtained from Animal Pharm Services Inc of Healdsburg, CA.

Solutions. Phosphate-buffered saline (PBS) contained 140 mM NaCl, 10 mM Na_2HPO_4, 3.4 mM KCl, 1.84 mM KH_2PO_4 (pH 7.3), and 5 mM EDTA. Lysis buffer consisted of 10 mM Tris-HCl (pH 7.5) and 0.5 mM $MgCl_2$. Buffer A included 300 mM NaCl, 10 mM Imidazole, 20% Glycerol, and 50 mM NaH_2PO_4. Buffer C contained 10 mM Tris-HCl (pH) 7.5), 300 mM NaCl, 25 mM Imidazole, and 0.1% *N*-dodecyl β-D-maltoside. Elution buffer consisted of 10 mM Tris-HCl (pH 7.5), 500 mM NaCl, 300 mM Imidazole, and 0.1% *N*-dodecyl β-D-maltoside. Tris medium included 50 mM Tris-HCl and 5 mM $MgCl_2$ (pH 7.4). Sample buffer (2×) contained 0.125M Tris-HCl, (pH 6.8), 4% SDS, 20% glycerol, and 50 mM DTT. Krebs Ringers Phosphate (KRP) consisted of 4.5% NaCl, 5.75% KCl, 7.85% $CaCl_2 \cdot H_2O$, 19.1% $MgSO_4 \cdot 7H2O$, and 0.1 M Na_2HPO_4.

Tissue Culture. HEK and Cos-7 cells were maintained in Dulbecco's Modified Eagle Medium (DMEM) supplemented with 10% FBS, 100 units/mL penicillin, and 100 μg/mL streptomycin in a 37 °C humidified 5% CO_2 incubator.

Polyacrylamide Gel Electrophoresis. Proteins were resolved on 10% acrylamide gels as described in ref *16*.

Western Blotting. Parental and recombinant GLUT1.HA.H_6 were detected by Western blot analysis. Peptides separated by SDS-PAGE were transferred electrophoretically to nitrocellulose membranes, which were subsequently blocked for 1 h in PBS-T (PBS + 0.1% Tween detergent) with 20% Carnation nonfat dry milk. Following four washes of 5 min in PBS-T, membranes were incubated for 1 h in primary antibody. C-Ab was diluted 1:10,000 in 3% nonfat dry milk/PBS-T, and HA-Ab was diluted to 1 μg/mL in 2% nonfat dry milk/PBS-T. Following four wash cycles to remove primary antibody, membranes were exposed for 45 min to secondary antibody (goat anti rabbit IgG, and goat anti-mouse IgG-horseradish peroxidase conjugates) diluted 1:5000 in PBS-T containing 3% or 2% nonfat dry milk. Detection of antigen−antibody complexes was achieved by chemiluminescence using Amersham ECL reagents.

Construction of Wild-Type and Mutant GLUT1-HA 6His. A 1.7 Kbp fragment of GluT1 cDNA was subcloned into the BamH1 cloning site of pGEM3Z (pGEM3Z-GT1)(*8*). Site-directed mutagenesis (Stratagene QuickChange^{tm} Kit) was used to introduce a unique Mfe1 restriction site at residue 1685 (GluT1 residue 491) in pGEM3Z-GT1. The HA-His6 epitope tag LYPYNVPNYAHHHHHH−STOP−STOP was inserted into the coding region of GluT1 at this location. The sequence of the tagged GluT1 was confirmed by sequence analysis (University of Massachusetts Medical School DNA sequencing laboratory). This tagged GluT1 construct was subcloned into the BamH1 site of the pcDNA3.1+ mammalian expression vector. The three putative ATP binding domains of GluT1 were subjected to alanine scanning mutagenesis. Mutants were engineered with the Stratagene QuickChange^{tm} Kit and confirmed by sequence analysis. GFP-tagged GluT1.HA.H_6 and GluT1$_{338-A}$ were constructed using the pEGFP−N3 expression vector (Clontech). BamH1 cloning sites were introduced into GluT1.HA.H_6 and GluT1$_{338-A}$ cDNAs immediately preceding the GluT1 stop site by using QuickChange. GluT1 BamH1 fragments were isolated and introduced into the MCS of pEGFP-N3. This results in in-frame additions of EGFP to the carboxyl-terminus of GluT1.HA.H_6 and GluT1$_{338-A}$, which were confirmed by sequencing. Expression of EGFP-tagged GluT1 in Cos-7 cells was confirmed by immunoblot analysis by using C-Ab, HA-Ab, and anti-GFP antibodies.

Transient Expression of Wild-Type and Mutant GluT1 in Cos-7 and HEK Cells. Subconfluent Cos-7 cells and HEK cells were transfected with wild-type and mutant GluT1.HA.H_6 cDNA using the Fugene 6 transfection reagent system. Following transfection, cells were maintained in DMEM for 24 h, at which time 0.72 mM G418 (Geneticin) was added to the media and the cells were allowed to continue growing for an additional 48 h. For harvesting, six culture plates of cells (150 mm) were washed twice with PBS + 5 mM EDTA and then scraped into 20 mL of lysis buffer mixed with 1 mM PMSF. Membranes were prepared according to (*17*). In brief, cells were homogenized for five minutes with a Fisher Dyna-Mix, then spun at 5000*g* for 10 min at 4 °C. The supernatant was decanted and centrifuged at 100 000*g* for 1 h to pellet crude membrane fractions. Membranes were resuspended in 300 μL Buffer A with 1 mM PMSF and frozen at −70 °C until use.

Purification of Wild-Type and Mutant GLUT1. Purification of recombinant GLUT1.HA.H_6 was as described in ref *18*. In brief, cell extracts were solubilized in 1.7 mL of solubilization buffer (buffer A + 1% *N*-dodecyl β-D-maltoside or octylglucoside) and then centrifuged at 15 000*g* for 15 min to remove insoluble material. The supernatant was allowed to bind for 1 h at 4 °C with 3 mL of Nickel−nitrilotriacetic acid (Ni−NTA) column media which had been preequilibrated with 8 mL of buffer B (buffer A + 0.1% *N*-dodecyl β-D-maltoside or octylglucoside). The column was washed twice with 8 mL of buffer B and twice with 8 mL of buffer C. Samples were eluted from the column with 2 mL of elution buffer and concentrated in centricon-10 concentrators.

Immunoblot analysis using HA-Ab and SDS-PAGE confirm that Ni−NTA chromatography results in the elution of His-tagged human GluT1. Densitometric analysis of immunoreactive material applied to and eluted from the column indicates that 40% of the applied His_6-tagged GluT1 is initially bound to the column. 33% of the bound GluT1 is retained during subsequent wash steps prior to displacement by addition of 300 mM imidazole.

Glucose Carrier Labeling with 8-Azido[γ-^{32}p]ATP. Labeling was carried out a described previously in ref *9*. A methanolic solution of 8-azido[γ-^{32}P]ATP was dried under nitrogen and resuspended in Tris medium at pH 7.4. Samples eluted from Ni−NTA were combined with the methanol-free 8-azido[γ-^{32}P]ATP solution (90 μCi ^{32}P, 5.5 μM final azidoATP concentration). The suspension was incubated on ice for 30 min to allow equilibrium azidoATP binding to GLUT1. Samples were placed on ice in separate wells of an ELISA dish and irradiated for 90 s at 280 nm in a Rayonet Photochemical Reactor. Following UV irradiation (photolabeling), samples were resolved on 10% SDS-PAGE gels and transferred electrophoretically to nitrocellulose membranes. Proteins labeled with 8-azido[γ-^{32}P]ATP were visualized by autoradiography and quantitated by densitometry.

2-Deoxy-D-glucose and 3MG Uptake in Cos-7 & HEK Cells Expressing Wild-Type and Mutant GLUT1-HA.His_6. Subconfluent Cos-7 cells and HEK cells in 12 well culture dishes were transfected with wild-type and mutant GluT1.HA.H_6 as described above. 2DOG or 3MG uptake (*8*) were measured 72 h post transfection at 37 °C. Prior to uptake, cells were serum starved in DME for 2 h at 37 °C. Cells were washed twice with KRP and then incubated at 4 or 37 °C for 15 min in KRP ± 10 μM CCB. Cells were exposed to 1 μCi/μL [^{3}H]2DOG or to 1 μCi/μL [^{3}H]3MG diluted 1:40 in KRP containing 0.1 mM unlabeled 2DOG or 3MG, respectively. Uptake was measured at several time points ranging from 5 s to 30 min and stopped by washing twice with 1 mL of ice cold KRP + CCB. Duplicate samples were counted following extraction with 450 μL 0.1% Triton-X100. Time zero uptake points were obtained by adding ice cold KRP to each well before the addition of medium containing sugar and radiolabel. Radioactivity associated with cell extracts at time zero was subtracted from the activity associated with cell extracts following the uptake period. All uptakes were normalized to Triton-X100-releasable cell protein. Uptake assays were performed using solutions and dishes preequilibrated to 4 or 37 °C.

Cytochalasin B Photolabeling. Membranes from Cos-7 cells transfected with GLUT1.HA.H_6, with mutant $GluT1_{332-3A}$, or with mutant $GluT1_{338-3A}$ were isolated as described previously for CHO cells (*8*). Samples were resuspended in 700 μL of 6.25 μM [^{3}H]-cytochalasin B (CCB) and 10 μM cytochalasin D ± 100 μM phloretin in PBS at pH 7.4 and allowed to equilibrate on ice for 10 min. This suspension was placed on ice and irradiated for 4 min at 280 nM in a Rayonet Photochemical Reactor. Following UV irradiation, membranes were washed with PBS to remove unbound CCB and sedimented by centrifugation (100 000*g* for 15 min). Proteins were resolved on 10% SDS PAGE gels and stained for protein or transferred to nitrocellulose for C-Ab and HA-Ab western blotting. Gel slices (2 mm) were extracted from stained gels and incubated overnight at 50 °C in 300 μL 30% H_2O_2 before addition of scintillation fluid and counting.

∂-Antibody Binding. Cos-7 cells were grown and transfected in 12 well culture dishes as previously described. ∂-Antibody binding was measured 72 h post transfection. Unless noted, all solutions were prewarmed to 37 °C. Cells were incubated for 1 h at 37 °C with sheep ∂-antibody diluted 1:1000 in DMEM +10% fetal bovine serum. Following two washes in KRP pH 7.4, cells were incubated for 30 min with [^{125}I]-protein G diluted 1:1200 in KRP. After two additional washes in KRP, duplicate samples were counted following extraction in 500 μL of 1% Triton in KRP pH 7.4. Protein G binding in the absence of primary antibody was used to quantitate background radioactivity and was subtracted from each sample. All measurements were normalized for total protein present in the culture well.

Fluorescence Microscopy. Preparation of cover slips and cell culture (Cos-7 cells) on cover slips were as described previously (*8*). Confocal fluorescence images were captured using an Olympus IX 70 Inverted Light microscope at the University of Massachusetts Medical School Digital Imaging Core Facility.

Data Analysis. Analysis of 8-bit densitometric scans of autoradiograms and immunoblots was carried out using NIH Image 1.62. Curve fitting by nonlinear regression was carried out using the software program Kaleidagraph v 3.51 (Synergy Software, Reading, PA).

RESULTS

Sugar Transport in Cos-7 and HEK Cells. Net uptake of 100 μM 2DOG at 37 °C by Cos-7 cells (Figure 1A) and net uptake of 100 μM 2DOG or 3MG by HEK cells at 37 °C (Figure 1B) proceed linearly for at least the first 30 min of cellular exposure to sugar (Figure 1). Sugar transport by both cell types is suppressed by the sugar transport inhibitor CCB (Figure 1). Uptake of 100 μM 2DOG (a metabolizable sugar) by HEK cells is some 5-fold more rapid than uptake of 100 μM 3MG (a nonmetabolizable sugar; Figure 1B). This may reflect the 4.4-fold higher affinity shown by human red cell GluT1 for 2DOG versus 3MG (*19*, *20*). 2DOG uptake by Cos-7 cells is some 6000-fold faster than 2DOG uptake by HEK cells (Figure 1). 3MG transport at 37 °C by Cos-7 cells is too fast to measure accurately using conventional sampling methods. Equilibration of intracellular water with extracellular 3MG is complete within 5 s (not shown). For these reasons, only 2DOG uptake by Cos-7 cells is reported here. The rate of 2DOG accumulation in Cos-7 cells is measurable because hexokinase-mediated 2DOG phosphorylation traps the radiolabeled sugar within the cell. It is likely, however,

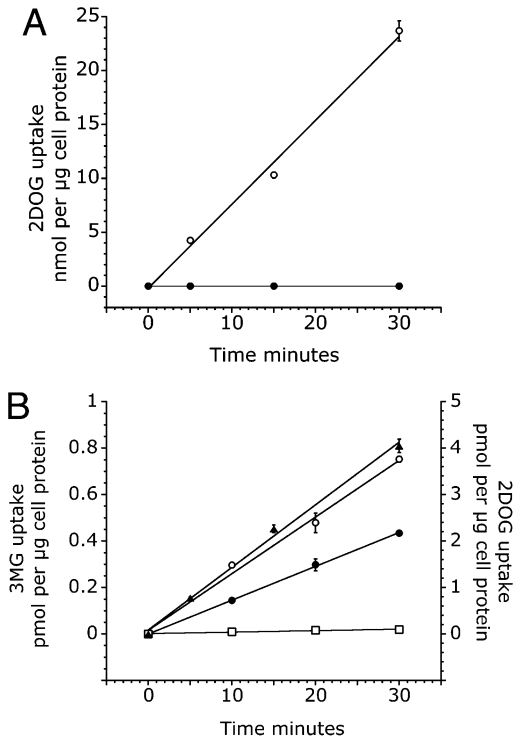

FIGURE 1: Sugar transport mediated by parental GluT1 in Cos-7 (A) and HEK (B) cells. (A) Ordinate: uptake of ^{3}H-2-deoxy-D-glycose (100 μM) in nmol per μg cell protein. Abscissa, time in minutes. Uptake was measure in quadruplicate at 37 °C in the absence (○) and presence (●) of the transport inhibitor CCB (10 μM). Each point shows the mean ± SEM of the determination. The straight lines drawn through the points were computed by linear regression and have the following slopes: control, 0.77 ± 0.03 nmol 2DOG per μg cell protein per min; CCB, 0.024 ± 0.003 nmol 2DOG per μg cell protein per min. (B) Ordinate: uptake of ^{3}H-3MG (100 μM; ○, ●, □) and ^{3}H-2DOG (100 μM; ▲) in pmol per μg cell protein. Abscissa, time in minutes. Uptake was measured in quadruplicate at 37 °C without (○, ▲) and with (●) prior treatment with FCCP (2 μg/mL) and NaCN (2 mM) for 2 h at 37 °C. Transport in unpoisoned cells was also measured in the presence of 10 μM CCB (□). Each point shows the mean ± SEM of the determination. The straight lines drawn through the points were computed by linear regression and have the following slopes: 3MG−control, 25.4 ± 1.3 fmol 3MG per μg cell protein per min; metabolic poisons, 14.6 ± 0.1 fmol 3MG per μg cell protein per min; control + CCB, 0.73 ± 0.07 fmol 3MG per μg cell protein per min; 2DOG−control, 134 ± 4 fmol 2DOG per μg cell protein per min.

that rates of 2DOG accumulation reported here provide a minimum estimate of the rate of 2DOG transport.

Immunoblot analysis of Cos-7 cell membranes suggests approximately 33 ng GluT1 per μg total membrane protein (3.3% GluT1 by mass). This compares with 5% GluT1 in human red cell membranes (*21*) and with approximately 0.3% GluT1 in HEK membranes (see Figure 2). While these analyses make simplifying assumptions of linearity in film response, identical cellular geometries and protein contents, and identical fractional cell surface expression of total cellular GluT1 in Cos-7 and HEK cells, the 10-fold difference in membrane GluT1 content contrasts starkly with the 6000-fold difference in cellular 2DOG transport rates.

However, a similar result is obtained upon comparison of GluT1-mediated sugar transport in red cells. 3MG net transport at 37 °C is at least 173 000-fold faster in human erythrocytes than in avian red cells, but human red cell GluT1 content is only 2000-fold greater (*22*). Sugar transport by avian red cells is suppressed under conditions of normal oxidative metabolism. We therefore exposed HEK cells to FCCP (2 μg/mL) and NaCN (2 mM) for 2 h to inhibit oxidative metabolism and examined the effects on net 3MG uptake. Table 1 shows that metabolic inhibition of HEK cells results in increased V_{max} and $K_{m(app)}$ for net 3MG uptake, but exchange transport (uptake by cells loaded with saturating 3MG (50 mM)) is unaffected.

Heterologous Expression of GluT1. Cell membranes isolated from Cos-7 cells transfected with hGluT1.HA.H_6 show a 2−3-fold increase in the expression of a 55 kDa C-Ab reactive protein relative to membranes isolated from non-transfected Cos-7 cells (Figure 2A). Plasma membranes were isolated from nontransfected- and hGluT1.HA.H_6-transfected Cos-7 cells and were treated with a high pH medium to remove peripheral membrane proteins. The remaining (presumed) integral membrane proteins were photolabeled using [γ-^{32}P]-azidoATP, resolved by SDS-PAGE, and subjected to quantitative autoradiography. Cos-7 cells expressing GluT1.HA.H_6 contain 3-fold more azidoATP-reactive proteins of average molecular mass 55 kDa than do nontransfected cells (Figure 2B).

To assess whether heterologously expressed wild-type and mutant hGluT1.HA.H_6 are functional, we measured 100 μM 2DOG uptake at 37 °C by Cos-7 cells transfected with wild-type or mutant hGluT1.HA.H_6 cDNA. Figure 3A shows that hGluT1.HA.H_6 transfected cells exhibit 1.7-fold greater levels of cytochalasin B (CCB) inhibitable 2DOG accumulation. This increase in net sugar uptake is consistent with the 2.4-fold increase in C-Ab-reactive protein expression observed in hGluT1.HA.H_6-transfected Cos-7 cells (Figure 2A) and with the 3-fold increase in azidoATP-labeled integral membrane proteins observed in hGluT1.HA.H_6-transfected Cos-7 cells (Figure 2B). This suggests that increased 2DOG uptake results from increased cell surface glucose transporter expression.

This hypothesis is further supported by the demonstration that cell surface binding of ∂-Ab (an antibody that interacts with exofacial epitopes of tetrameric GluT1; *8*, *23*) is increased 2.1-fold upon Cos-7 cell transfection with hGluT1.HA.H_6 (Figure 3B). These transport measurements were made at subsaturating sugar concentrations where (assuming simple, saturable transport) the rate of uptake is proportional to the ratio $V_{max}/K_{m(app)}$ (V_{max} is the cellular sugar transport capacity, and $K_{m(app)}$ is that 2DOG concentration at which uptake is one-half V_{max}). Since increased 2DOG transport is proportional to the increase in cell surface GluT1 expression, this suggests that $K_{m(app)}$ for GluT1-mediated 2DOG transport in Cos-7 cells is not grossly perturbed by introduction of a carboxyl-terminal HA.H_6 epitope tag.

Figure 3A compares uptake of 2DOG by control and transfected Cos-7 cells expressing hGluT1.HA.H_6 or GluT1 alanine mutants. In most instances, 2DOG transport by GluT1 alanine mutants is comparable to hGluT1.HA.H_6-mediated transport. One exception is mutant $GluT1_{338-3A}$, which fails to increase 2DOG uptake beyond parental levels. This could result from failure of $GluT1_{338-3A}$ to reach the cell surface. Analysis of ∂-Ab (cell surface GluT1) and HA-Ab and C-Ab (total GluT1 content) binding confirms $GluT1_{338-3A}$ expression but suggests either that the mutant does not reach the cell surface or that the mutant does not assemble as a tetramer (Figure 3B). cDNAs encoding hGluT1.HA.H_6 and

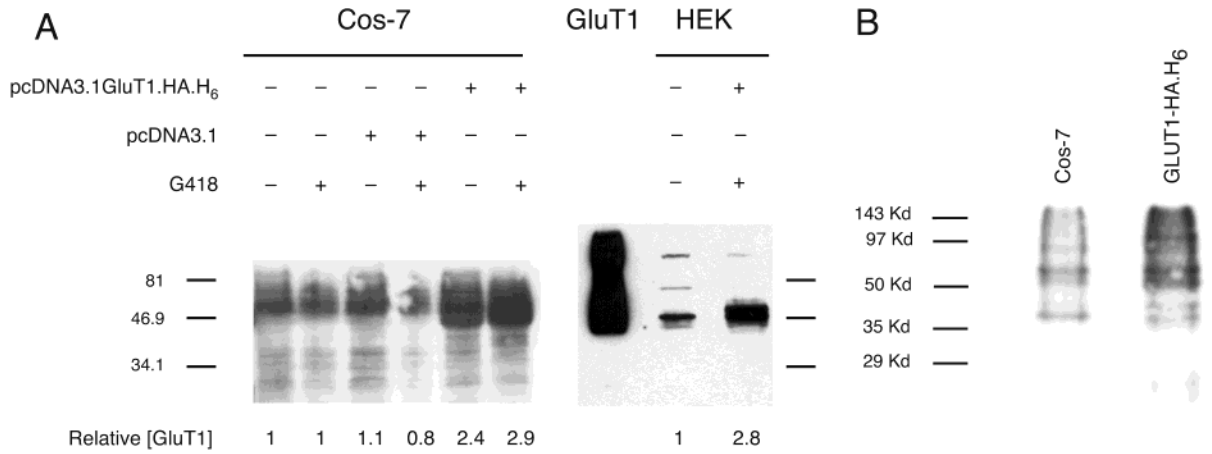

FIGURE 2: Expression of GluT1 in Cos-7 and HEK cells. (A) C-Ab immunoblot analysis of parental and GluT1.HA.H_6 expressed in Cos-7 cells indicates that total cellular GluT1 content is increased by 2.4−2.9-fold by transfection with pcDNA3.1-GluT1.HA.H_6. Inclusion of G418 in the growth medium, transfection of cells with vector lacking GluT1.HA.H_6 cDNA (pcDNA3.1), and transfection of cells with vector containing GluT1.HA.H_6 cDNA (pcDNA3.1+ GluT1.HA.H_6) are indicated above the lanes of the autoradiogram. Quantitative densitometry using NIH Image was used to determine GluT1 expression levels. The results are shown below the autoradiogram assuming that GluT1 expression in Cos-7 cells in the absence of G418 represents 1 unit of expression. The mobility of molecular weight markers is shown to the left and right of the autoradiogram. Results are also shown for purified GluT1 (2.5 μg) and for parental GluT1 and GluT1.HA.H_6 expression in HEK cells. (B) [γ-^{32}P]-AzidoATP labeling of Cos-7 cell membranes depleted of peripheral membrane proteins. Isolated Cos-7 cell membranes from control cells or from cells transfected with GLUT1.HA.H_6 were labeled with azidoATP following removal of peripheral proteins by a single alkaline wash. Samples were resolved on 10% SDS-PAGE gels and transferred to nitrocellulose. Protein contents were determined using a Pierce BCA assay kit, and 35 μg of total protein was loaded in each lane. Label incorporation was detected by exposure of membranes to autoradiographic film. AzidoATP binding was quantitated by densitometry using NIH Image. Membranes from GluT1.HA.H_6 transfected cells contain 3-fold more azidoATP label than membranes isolated from nontransfected cells.

Table 1: Effects of Metabolic Stress on 3MG Transport in Cells

	control cells			metabolically depleted[a]		
cells	$K_{m(app)}$[b]	V_{max}[c]	exchange[d]	$K_{m(app)}$[b]	V_{max}[c]	exchange[d]
human red cells	0.38 ± 0.02	113 ± 11	5410 ± 224	13.2 ± 1.0	1234 ± 78	4876 ± 279
HEK cells	0.65 ± 0.1	256 ± 46.5	1095 ± 77	3.5 ± 0.4	974 ± 66	990 ± 7

[a] Cells were ATP-depleted by ghosting (red cells) or by exposure to 2 mM NaCN + 2 μg/mL FCCP for 2 h. [b] $K_{m(app)}$ for net uptake in mM. [c] V_{max} for net uptake was measured as μmol/L cell water/ min (red cells) or fmol/μg protein/min (HEK cells). [d] Equilibrium exchange V_{max} describes saturated unidirectional sugar uptake into cells containing saturating [3MG] and has the same units as V_{max} for net uptake. With HEK cells, full concentration dependence of exchange sugar transport is not available. Uptake was measured at 100 μM 3MG into cells equilibrated with 50 mM unlabeled 3MG. Units are as for net uptake. Data are shown as the mean ± SEM of the results of at least 3 separate experiments.

hGLUT1$_{338-3A}$ were packaged into the multiple cloning site of pEGFP−N3. The resulting in-frame additions of EGFP coding sequence to the carboxyl-terminus of GluT1.HA.H6 and GluT1$_{338-A}$ were confirmed by DNA sequencing. Cos-7 cells were transfected with these vectors and analyzed for plasma membrane GFP content by fluorescence microscopy. 3-D image stacks of fluorescent cells were acquired and were subjected to digital deconvolution by using the exhaustive photon reassignment (EPR) algorithm (*24*). Our results strongly suggest (Figure 4A) that GFP-tagged hGluT1.HA.H_6 and GluT1$_{338-3A}$ are expressed at the cell surface. We hypothesize that hGluT1$_{338-3A}$ is targeted appropriately but is catalytically impaired.

hGluT1.HA.H_6 photolabeling experiments (Figure 4B) using [^{3}H]-CCB (a membrane-permeant, sugar export site ligand) show that membranes isolated from Cos-7 cells transfected with hGluT1.HA.H_6 or with GluT1$_{332-3A}$ (a transport normal mutant) show 2−3-fold greater phloretin-inhibitable [^{3}H]-CCB photoincorporation into GluT1 than do membranes isolated from control cells or from cells transfected with GluT1$_{338-3A}$. These results suggest that Glut1$_{338-3A}$ is also dysfunctional with respect to CCB binding.

Effects of Cellular Metabolic Depletion on Sugar Transport by Cells Expressing Heterologous GluT1. As with 3MG transport in human red blood cells (*25*), V_{max} and $K_{m(app)}$ for net sugar uptake in nontransfected HEK cells are increased upon cellular ATP depletion. Table 1 shows that HEK cell treatment with 2 μg/mL FCCP for 2 h increases V_{max} and $K_{m(app)}$ 3MG uptake at 37 °C by 3- and 5.6-fold, respectively. It is not possible to accurately assess the effects of metabolic inhibition on sugar transport in Cos-7 cells because ATP depletion may affect the rate of 2DOG phosphorylation by hexokinase.

GluT1.HA.H_6 expression in HEK cells (Figure 2) results in a 3-fold increase in 100 μM 3MG net uptake at 37 °C (Figure 5). Similar increases in net 3MG transport are also observed in HEK cells transfected with GluT1$_{332-3A}$, GluT1$_{E329-D}$, and GluT1$_{E329-A}$ (Figure 5). Exposure to FCCP results in net inhibition of 100 μM 3MG uptake by HEK cells expressing parental GluT1 and parental GluT1 + GluT1.HA.H_6 (Figures 1B and 5). This is expected because transport at fixed, subsaturating [3MG] (e.g., 100 μM) is directly proportional to the constant $V_{max}/K_{m(app)}$ and FCCP acts to reduce $V_{max}/K_{m(app)}$ for GluT1-mediated transport in HEK cells (Table 1). Although HEK cells expressing GluT1$_{332-3A}$ show high rates of CCB-inhibitable net sugar uptake consistent with increased cellular GluT1 content, these cells fail to respond to FCCP with reduced net sugar uptake

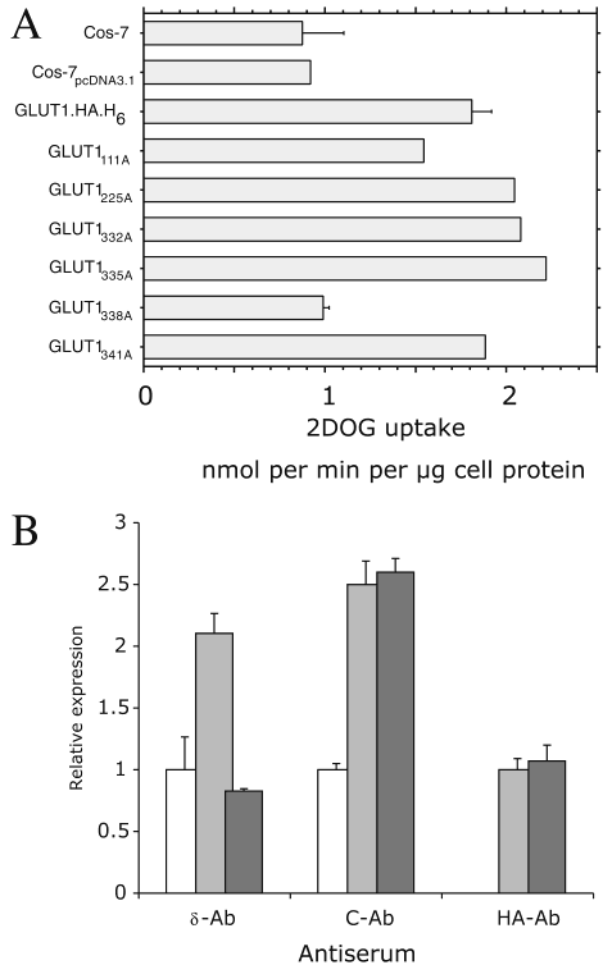

FIGURE 3: (A) Comparison of 2DOG (0.1 mM) uptake at 37 °C by Cos-7 cells, Cos-7 cells transfected with vector (pcDNA3.1) lacking GluT1 sequence, and Cos-7 cells expressing GluT1.HA.H_6 and GluT1.HA.H_6 alanine mutants. Ordinate: CCB-inhibitable 2DOG accumulation (nmol per min per μg total cell protein). Abscissa: cells in which transport was measured. Results are shown as mean ± SEM of triplicate measurements. (B) Antibody binding to Cos-7 cells expressing parental GluT1 (white bars) parental GluT1+GluT1.HA.H_6 (gray bars) and parental GluT1 + $GluT1_{338-3A}$ (black bars). Ordinate, relative IgG binding; abscissa, IgG binding measured. Results are shown as mean ± SEM of three measurements made in duplicate. With ∂-Ab and C-Ab, binding is expressed relative to binding in nontransfected Cos-7 cells. With HA-Ab, binding is expressed relative to cells expressing parental GluT1+ GluT1.HA.H_6. ∂-Ab binding was measured in intact cells. C-Ab and HA-Ab reactivity was measured by immunoblot analysis of cell membranes isolated from Cos-7 cells.

(Figure 5). A similar result is obtained with $GluT1_{329E-A}$, but $GluT1_{329E-D}$ resembles hGluT1.HA.H_6 and parental GluT1 in its response to FCCP-poisoning.

Photolabeling Wild-Type and Mutant GluT1 with AzidoATP. The site(s) of GluT1 photoincorporation of azidoATP include(s) a domain extending from GluT1 residues 301−364 (*9*). This region of GluT1 also contains primary sequence (residues 332−343) that is 50% identical to a region of adenylate kinase that flanks the adenine ribose moiety and triphosphate chain of Mg.ATP (*15*). We therefore examined photoincorporation of [γ-^{32}P]azidoATP into GluT1.HA.H_6 and into alanine mutants of GluT1.HA.H_6, in which the primary structure of this adenylate kinase ATP binding homology domain is perturbed. We also modified the putative GluT1 Walker A motif (residues 111−117) and AKHD2 (residues 225−229) that lies in the large, middle cytoplasmic loop of GluT1.

Transiently expressed, detergent-solubilized hGluT1.HA.H_6 and hGluT1-alanine mutants were isolated by Ni−NTA affinity chromatography, concentrated by filtration centrifugation, and then photolabeled by using 10−15 μM [γ-^{32}P]-azidoATP. The presence of detergent is without effect on azidoATP photolabeling of isolated human red blood cell GluT1[1]. Labeled proteins were resolved by SDS PAGE and transferred to nitrocellulose. Two of three nitrocellulose membranes were used for C-Ab and HA-Ab immunoblot analysis (Figure 6A). The third membrane containing azidoATP photolabeled GluT1 was exposed to film for 5−24 h (Figure 6A). GluT1 expression and azidoATP photoincorporation were quantitated by densitometry, and the ratio {azidoATP-photoreactive protein:HA-Ab reactive protein} was computed to facilitate data normalization between experiments. With the exception of GluT1 constructs $GluT1_{329E-A}$ and $GluT1_{332-3A}$, the ratio {photolabel incorporation:HA-Ab staining} is constant for all alanine mutants and hGluT1.HA.H_6 (Table 2). $GluT1_{332-3A}$ and $GluT1_{329E-A}$ show increased {photolabel incorporation:HA-Ab staining} ratios by 2.5−11-fold (Table 2 and Figure 6A). Photolabel incorporation into $GluT1_{329E-D}$ and hGluT1.HA.H_6 are indistinguishable.

hGluT1.HA.H_6 and $GluT1_{332-3A}$ were subjected to competition analysis of ATP-inhibition of azidoATP photoincorporation. Affinity-purified hGluT1.HA.H_6 and $Glut1_{332-3A}$ were photolabeled using azidoATP in the presence of increasing concentrations of unlabeled ATP. As with azidoATP-photolabeling of isolated purified human erythrocyte glucose transport protein (*5*, *9*), photoincorporation of azido ATP into affinity purified hGluT1.HA.H_6, and $Glut1_{332-3A}$ is inhibited half-maximally by 50−150 μM ATP (Figure 6B). With $Glut1_{332-3A}$, however, photoincorporation of azidoATP in the absence of ATP is some 10-fold greater.

DISCUSSION

GluT1-mediated sugar transport by human red blood cells is modulated by intracellular ATP (*4*, *7*). ATP interacts directly with GluT1 (*5*) to reduce both $K_{m(app)}$ and V_{max} for net 3MG uptake and to reduce V_{max} but increase $K_{m(app)}$ for net exit (*26*, *27*). Transport inhibition by ATP is reconstituted in vitro using purified GluT1 proteoliposomes (*9*, *10*) and non-hydrolyzable analogues of ATP (*6*), indicating that inhibition is a direct consequence of ATP binding to GluT1. Red cell glucose transport is also inhibited by isoflavone tyrosine kinase inhibitors and other phytoestrogens (*28*, *29*) which interact at an endofacial (estrogen binding) GluT1 site (*30*). ATP competitively anatagonizes estradiol and genistein inhibitions of glucose exit from red cells (*29*), suggesting that GluT1 nucleotide and estrogen binding sites overlap or are mutually exclusive. Accordingly, it has been proposed that GluT1 ATP and estrogen binding sites share common sequence (*13*, *28*).

This hypothesis has gained support from recent comparisons (*29*) of the ligand-binding domain of the estrogen receptor β(esr-2) (*31*) with sequence of GluT1 hydrophilic, putative, nucleotide binding domains (*9*). The available data suggest a potential estrogen binding site between GluT1 cytoplasmic residues Glu_{326}, Arg_{327}, and His_{334} (*29*). This

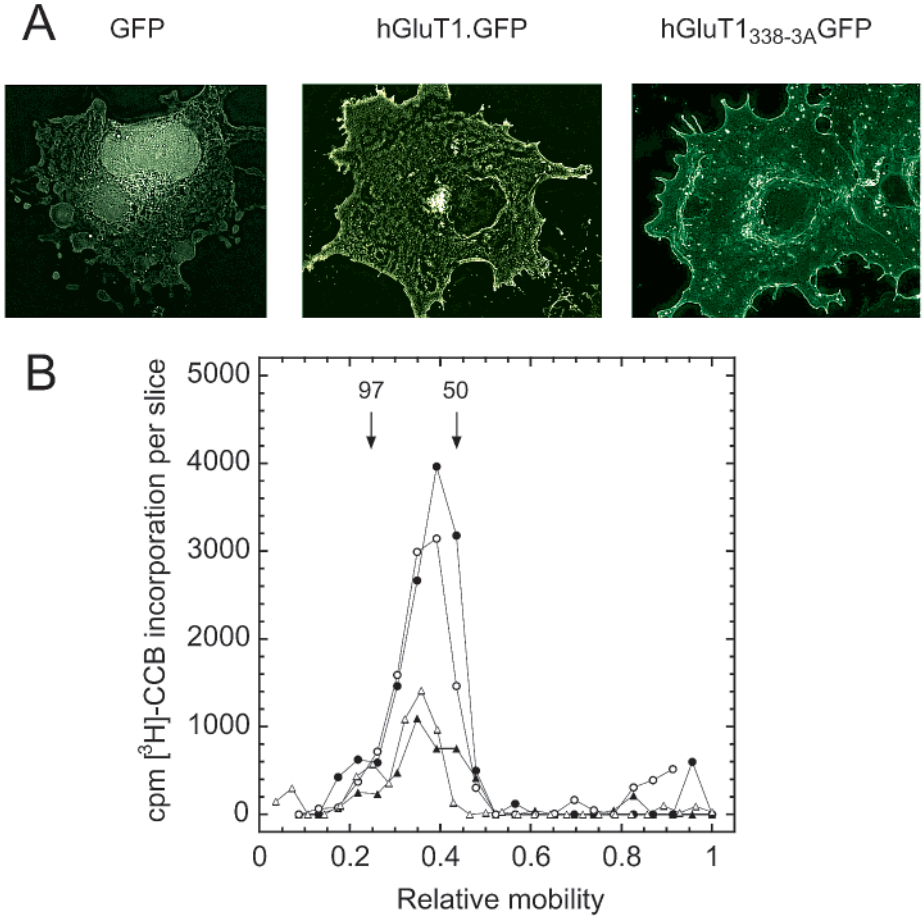

FIGURE 4: (A) Localization of GFP-tagged wild-type GluT1 and GFP-tagged $GluT1_{338-3A}$ transiently expressed in Cos-7 cells as detected by fluorescence microscopy. Nontransfected, GFP-tagged wild-type GluT1, and GFP-tagged $GluT1_{338-3A}$ transfected cells were grown on cover slips and analyzed for GFP fluorescence by fluorescence microscopy. 3-D image stacks of fluorescent cells were acquired and were subjected to digital deconvolution by using the exhaustive photon reassignment (EPR) algorithm (*24*). (B**)** Photolabeling of parental GluT1 and transfected wild-type and mutant human GluT1 in Cos-7 cells by the sugar export site ligand [^{3}H]-CCB. Cos-7 cell membranes were photolabeled in the presence and absence of 100 μM phloretin. Membranes were washed to remove unincorporated [^{3}H]-CCB, and membrane proteins were separated by SDS−Page. Following Coomassie staining, each gel lane was sliced into 2 mm sections, dissolved, and counted for associated [^{3}H]-CCB. Ordinate: phloretin-inhibitable CCB incorporation (cpm). Abscissa: relative mobility (gel slice number divided by total number of gel slices). Key: (△) nontransfected Cos-7 cell membranes (50 μg protein); (●) membranes (50 μg protein) from Cos-7 cells transfected with GluT1.HA.H_6; (○) membranes (50 μg protein) from cells transfected with $GluT1_{332-3A}$; (▲) membranes (50 μg protein) from Cos-7 cells transfected with $GluT1_{338-3A}$.

region of the glucose transporter is homologous to an adenylate kinase ATP binding domain that flanks the adenine ribose and triphosphate chain of liganded Mg.ATP in adenylate kinase (*15*). This region also includes the cytosolic, hydrophilic portion (residues 329−337) of a labeled peptide (residues 301−368) obtained upon proteolysis of azidoATP labeled GluT1 (*9*).

The accompanying study (*10*) demonstrates that the glucose transporter presents multiple, cooperative nucleotide binding sites. The nucleotide-free glucose transporter displays reduced affinity for ATP relative to transporter containing bound nucleotide. As pH is reduced from 7.4 to 6, the transporter now presents high-affinity ATP binding sites in the absence of nucleotide and occupancy by one or two molecules of ATP exposes additional nucleotide binding sites (*10*). We hypothesize that the carrier presents multiple, cooperative nucleotide binding sites because it is comprised of four identical, interacting subunits (GluT1 protein; *8*, *23*), each of which presents a single nucleotide binding site.

How does ATP binding enhance subsequent nucleotide binding affinity and how does reduced pH amplify this effect? In the absence of detailed structures of GluT1 with and without complexed nucleotide, answers to these questions are dependent upon indirect evidence. Stopped-flow fluorescence measurements of TNP-ATP binding to GluT1 indicate that the second-order rate constant for nucleotide association with nucleotide-complexed carrier is not accelerated relative to that for TNP-ATP binding to apoGluT1 (*10*). Rather, it is the nucleotide•GluT1 dissociation step that is inhibited 16-fold by GluT1 occupancy by TNP-ATP. The subunit−subunit interactions inhibiting nucleotide dissociation are unknown.

pH-sensitive nucleotide binding over the pH range 6−7.4 is consistent with involvement of a histidine side chain in nucleotide binding. Previous studies have ruled out chelation of ATP by H^+ as the causal factor in enhanced ATP binding to GluT1 at low pH (*9*). GluT1 contains five histidine residues, of which four (H160, 239, 337, and 484) are located within cytoplasmic domains. Exofacial His_{50} is an unlikely candidate since red cell sugar transport is insensitive to altered extracellular pH (*12*). His_{337} lies within the intracellular portion of the GluT1 ATP binding domain (residues

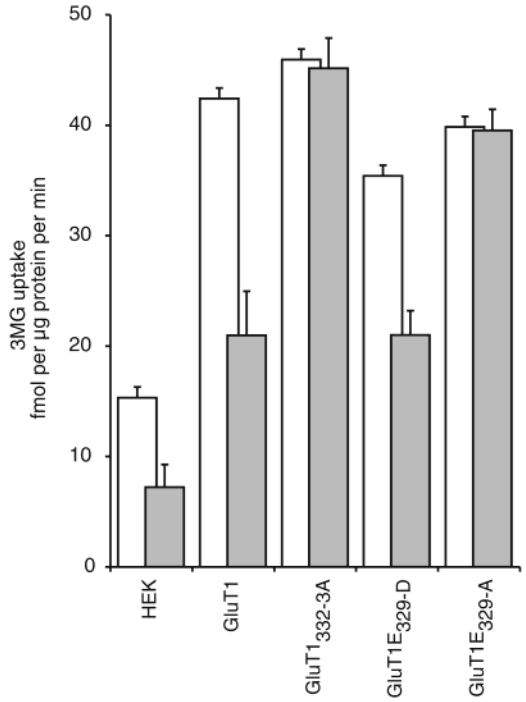

FIGURE 5: Effects of 2 h exposure at 37 °C to FCCP (2 μg/mL) on 3MG (100 μM) uptake by HEK cells at 37 °C. GluT1.HA.H_6 and GluT1.HA.H_6 alanine mutants were transiently expressed in HEK cells. Two days post transfection, cells were exposed to serum-free saline with (gray bars) or without (white bars) 2 μg/mL FCCP for 2 h before the uptake of 3MG was measured at 37 °C over intervals of 0, 5, 15, and 30 min (during which time uptake increases linearly with time). Results are shown as mean ± SEM of at least three separate determinations. Ordinate: 3MG uptake (fmol per μg protein per minute). Abscissa: cells in which uptake was measured. Key: HEK, nontransfected cells; GluT1, HEK cells transfected with GluT1.HA.H_6; $GluT1_{332-3A}$, HEK cells transfected with $GluT1_{332-3A}$; $GluT1_{E329-D}$, HEK cells transfected with $GluT1_{E329-D}$; $GluT1_{E329-A}$, HEK cells transfected with $GluT1_{E329-A}$

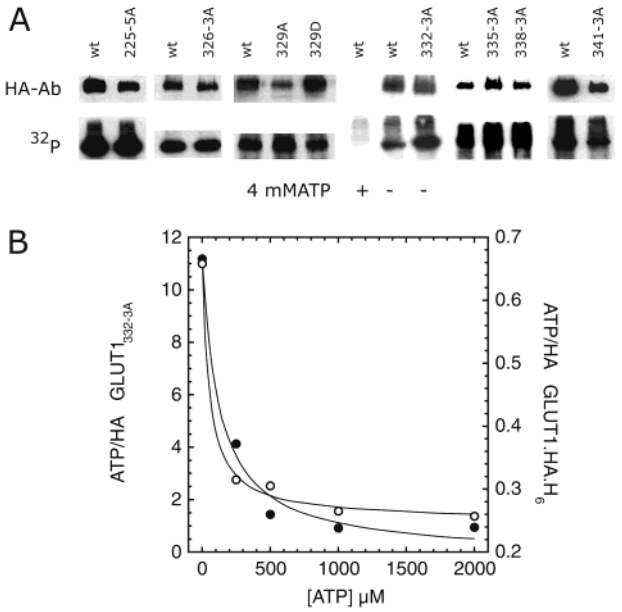

FIGURE 6: [γ-^{32}P] Azido ATP labeling of GLUT1.HA.H_6 and several of its corresponding alanine mutants. (A) Transporter was purified by Ni−NTA affinity chromatography of membranes isolated from Cos-7 cells transfected with wild-type or mutant GluT1.HA.H_6. Purified GluT1 was photolabeled using 10 μM [γ-^{32}P]-azidoATP, resolved on three separate 10% SDS PAGE gels (25 μg total protein per lane per gel), and transferred to nitrocellulose for western blotting and autoradiography. For each group of mutants, an internal control of GluT1.HA.H_6 was also processed. Control protein is visible at the far left of each group of blots. GluT1 constructs were identified by C-Ab and HA-Ab immunoblot analysis. Incorporated affinity label (azidoATP) was detected by autoradiography. Antibody and ATP binding were quantitated by densitometry using NIH Image. (+ ATP) shows that Ni−NTA purified GluT1.HA.H_6 photolabeling by azidoATP is inhibited in the presence of 4 mM unlabeled ATP. (B) ATP inhibition of azidoATP photolabeling of affinity purified GluT1.HA.H_6 (○) and $GluT1_{332-3A}$ (●). Purified, epitope-tagged GluT1 was photolabeled as in Figure 6A in the presence of increasing unlabeled [ATP]. Proteins were resolved by SDSPAGE and label incorporation, and epitope-tagged GluT1 was quantitated by densitometry of ^{32}P-autoradiograms and HA-Ab immunoblots. Ordinate: the ratio [^{32}P]-incorporation:HA-Ab reactivity. Abscissa: [ATP] present during photolabeling in μM. Curves drawn through the points were computed by nonlinear regression assuming that inhibition of photolabeling shows simple saturation kinetics and is characterized by the expression: labeling $= N - P[\text{ATP}]/K_{i(\text{app})} + [\text{ATP}]$ where N is label incorporation in the absence of unlabeled ATP, P is the amount by which saturating unlabeled ATP inhibits label incorporation, and $K_{i(\text{app})}$ is that concentration of unlabeled ATP which reduces labeling by 50%. The following constants were obtained: GluT1.HA.H_6, $N = 0.66 \pm 0.01$, $P = 0.41 \pm 0.04$, $K_{i(\text{app})} = 127 \pm 49$ μM ATP; $GluT1_{332-3A}$, $N = 11.2 \pm 0.7$, $P = 11.3 \pm 1.0$, $K_{i(\text{app})} = 54 \pm 17$ μM ATP. This figure summarizes three paired experiments.

301−361) identified by N-terminal sequence analysis of proteolytic fragments obtained from azidoATP-labeled GluT1 (*9*). Protonation of His_{337} could enhance ATP binding directly by increasing ionic interaction between ATP and His^+ within the binding pocket. Alternatively, protonated His_{337} might participate in a cation-π interaction (*32*) with, for example, Phe_{326} or could interfere with a cation-π interactions through ionic repulsion of cation-bearing side chains (e.g., Arg_{330}, Arg_{333}, or Arg_{334}). Alanine substitutions of His_{337} and Phe_{326} are without effect on azidoATP labeling of GluT1, suggesting that these residues do not play a pivotal role in nucleotide binding to GluT1. On the other hand, alanine substitutions of Glu_{329} and of the triplet $_{332}GRR_{334}$ enhance azidoATP photoincorporation into GluT1 and block modulation of recombinant GluT1-mediated sugar transport by cellular metabolic depletion. Aspartate substitution of Glu_{329} produces a wild-type GluT1 phenotype with respect to azidoATP labeling and sugar transport modulation.

These findings are consistent with the hypothesis that GluT1 contains a proton-sensitive saltbridge (Glu_{329}−$Arg_{333/334}$) within a component of the ATP binding domain. When this putative bridge is disrupted (by propagation of an ATP binding induced subunit conformational change to neighboring subunits or, by lowered pH or, by mutagenesis), the ATP binding affinities of the remaining subunits are increased significantly (bound ATP dissociates less rapidly), resulting in enhanced ATP binding. Thus, lowered pH reduces $K_{d(\text{app})}$ for binding of TNP-ATP (an ATP analog) to GluT1 from 530 μM (pH 7.4) to 120 μM (pH 6; *10*).

Glycine substitution of all three arginine residues of the GluT1 motif R-X-G-R-R (GluT1 residues 330−334) results in mis-folded GluT1 with no detectable activity in Xenopus oocytes (*33*). Our studies suggest that R_{330} is the critical residue because $GluT1_{332-3A}$ transports sugar efficiently when expressed in Cos-7 and HEK cells. In contrast, Liu et al. (*13*) report that alanine substitution of Gly_{332} results in 5-fold lower GluT1 transport activity when expressed in *Xenopus* oocytes. In the same studies, alanine substitutions at residues

Table 2: Effects of GluT1 Mutagenesis on Azido ATP Photoincorporation

GluT1 construct[a]	relative azidoATP incorporation[b]
GluT1.HA.H_6	1
$GluT1_{111-4A}$	1.21
$GluT1_{225-5A}$	1.75 ± 0.3
$GluT1_{326A}$	1
$GluT1_{329A}$	2.6 ± 0.6
$GluT1_{329D}$	0.98 ± 0.16
$GluT1_{332-3A}$	6.7 ± 1.6
$GluT1_{335-3A}$	0.84
$GluT1_{338-3A}$	1.14
$GluT1_{341-3A}$	0.86
$GluT1_{337A}$	1

[a] The core GluT1 construct encodes for wild-type human GluT1 with the C-terminal extension of an HA epitope (LYPYNVPNYA) terminating in six histidine residues. Subscripts indicate the nature and location of the introduced mutation(s). For example, in $GluT1_{111-4A}$, beginning at residue 111, four consecutive residues are replaced with Ala. For point mutations, the residue and the identity of the substitution are shown. For example, with $GluT1_{329A}$, residue 329 (Glu) is replaced with Ala. [b] [γ-^{32}P]AzidoATP incorporation into affinity purified transporter was quantitated by densitometry as the ratio of [γ-^{32}P]:α-HA antibody-reactive protein. Results are shown relative to GluT1.HA.H_6 (1.0) and, where three or more separate determinations were made, are indicated as mean $\pm$ SEM.

111 and 336 were, as in our hands, without effect on net transport. Studies with GluT4 expressed in and reconstituted from Cos-7 cells (*34*) demonstrate reduced sugar transport when residues corresponding to human GluT1 Arg_{333} and Arg_{334} were mutagenized to leucine and alanine, respectively. Binding of exo- and endofacial ligands to plasma membranes containing this mutant GluT4 was unaffected. These data contrast with our work showing normal transport activity but altered ATP binding in $GluT1_{332-3A}$ and may be isoform-specific (GluT4 is insensitive to ATP, *35*), may result from our use of alanine rather than leucine at position 333, or may be related to the method of transport measurement. Our experiments measure sugar transport across the plasma membrane of intact Cos-7 cells. The GluT4 studies were carried out by reconstitution of total membrane GluT4 into proteoliposomes. Substitution of residues 333−334 results in the loss of two of the three charged side chains thought to be important for establishing normal GluT1 membrane topography (*33*). In the absence of this determinant, $GluT4_{333/334LA}$ may lose topographical integrity when exposed to detergents during reconstitution (e.g., see ref *36*). Thus reconstituted, mutant protein might be dysfunctional while plasma membrane-resident protein retains normal function.

Can this model account for variable acute cellular sugar transport responses to metabolic challenge? Some GluT1 expressing cells respond to metabolic depletion with rapid acceleration of net sugar transport resulting from increased catalytic turnover of GluT1 (*4*, *7*, *22*, *27*, *37*−*39*). Some GluT1-expressing cells are, however, unresponsive to cellular metabolic insult (*40*, *41*).

Red cell sugar transport sensitivity to physiologic, saturating [ATP] is lost at lowered pH (*9*). Paradoxically, ATP sensing (binding) is enhanced under these conditions. We propose that when unoccupied by ATP, the carrier behaves as a low-affinity, high-capacity transporter in which the cytosolic gate to the internal occlusion cage is open more frequently than it is closed (*10*). When one or two subunits of tetrameric GluT1 are complexed with ATP, the transporter behaves as if a high-affinity, low-capacity carrier (the gate to the occlusion cage closes more frequently or is closed for longer intervals). As the remaining two subunits become complexed with ATP, the gate now opens more frequently, and the carrier behaves as if it were in the nucleotide-free, low-affinity high-capacity state. This could explain why $GluT1_{332-3A}$ and $GluT1_{329E-A}$ are unresponsive to cellular metabolic perturbation. This conclusion also requires (given the levels of GluT1 expression observed in these studies) that when complexed with parental wild-type GluT1, the heteroGluT1 complex (e.g., a GluT1−$GluT1_{332-3A}$ complex) behaves as if comprised only of $GluT1_{332-3A}$.

CONCLUSIONS

Our studies demonstrate that ATP binding to and regulation of GluT1-mediated sugar transport is sensitive to pH and to mutagenesis at GluT1 residue 329 and 333/334. We propose that cooperative nucleotide binding to tetrameric GluT1 is controlled by a proton-sensitive, intracellular saltbridge (Glu_{329}−$Arg_{333/334}$) present in each GluT1 subunit. The net effect of ATP binding on GluT1-mediated sugar transport is determined by the number of ATP molecules liganded to the transporter complex. This hypothesis may explain differential acute cellular responses to metabolic distress.

REFERENCES

1. Kasahara, M., and Hinkle, P. C. (1977) Reconstitution and purification of the D-glucose transporter from human erythrocytes, *J. Biol. Chem. 253*, 7384−7390.
2. Zoccoli, M. A., Baldwin, S. A., and Lienhard, G. E. (1978) The monosaccharide transport system of the human erythrocyte. Solubilization and characterization on the basis of cytochalasin B binding, *J. Biol. Chem. 253*, 6923−6930.
3. Mueckler, M., Caruso, C., Baldwin, S. A., Panico, M., Blench, I., Morris, H. R., Allard, W. J., Lienhard, G. E., and Lodish, H. F. (1985) Sequence and structure of a human glucose transporter, *Science 229*, 941−945.
4. Hebert, D. N., and Carruthers, A. (1986) Direct evidence for ATP modulation of sugar transport in human erythrocyte ghosts, *J. Biol. Chem. 261*, 10093−10099.
5. Carruthers, A., and Helgerson, A. L. (1989) The human erythrocyte sugar transporter is also a nucleotide binding protein, *Biochemistry 28*, 8337−8346.
6. Heard, K. S., Fidyk, N., and Carruthers, A. (2000) ATP-dependent substrate occlusion by the human erythrocyte sugar transporter, *Biochemistry 39*, 3005−3014.
7. Helgerson, A. L., Hebert, D. N., Naderi, S., and Carruthers, A. (1989) Characterization of two independent modes of action of ATP on human erythrocyte sugar transport, *Biochemistry 28*, 6410−6417.
8. Zottola, R. J., Cloherty, E. K., Coderre, P. E., Hansen, A., Hebert, D. N., and Carruthers, A. (1995) Glucose transporter function is controlled by transporter oligomeric structure. A single, intramolecular disulfide promotes GLUT1 tetramerization, *Biochemistry 34*, 9734−47.
9. Levine, K. B., Cloherty, E. K., Fidyk, N. J., and Carruthers, A. (1998) Structural and physiologic determinants of human erythrocyte sugar transport regulation by adenosine triphosphate, *Biochemistry 37*, 12221−32.
10. Cloherty, E. K., Levine, K., Graybill, C., and Carruthers, A. (2002) Cooperative nucleotide binding to the human erythrocyte sugar transporter, *Biochemistry 41*, 12639−12651.
11. Coderre, P. E., Cloherty, E. K., Zottola, R. J., and Carruthers, A. (1995) Rapid substrate translocation by the multi-subunit, erythroid glucose transporter requires subunit associations but not cooperative ligand binding, *Biochemistry 34*, 9762−9773.
12. Sen, A. K., and Widdas, W. F. (1962) Determination of the temperature and pH dependence of glucose transfer across the

human erythrocyte membrane measured by glucose exit, *J. Physiol. 160*, 392−403.
13. Liu, Q., Vera, J. C., Peng, H., and Golde, D. W. (2001) The predicted atp-binding domains in the hexose transporter glut1 critically affect transporter activity, *Biochemistry 40*, 7874−81.
14. Hresko, R. C., Kruse, M., Strube, M., and Mueckler, M. (1994) Topology of the Glut 1 glucose transporter deduced from glycosylation scanning mutagenesis, *J. Biol. Chem. 269*, 20482−8.
15. Fry, D. C., Kuby, S. A., and Mildvan, A. S. (1986) ATP-binding site of adenylate kinase: Mechanistic implications of its homology with ras-encoded p21, F1-ATPase, and other nucleotide-binding proteins,*Proc. Natl. Acad. Sci. U.S.A. 83*, 907−911.
16. Laemmli, U. K. (1970) *Nature 270*, 680−685.
17. Loo, T. W., and Clarke, D. M. (1993) Functional consequences of proline mutations in the predicted transmembrane domain of P-glycoprotein, *J. Biol. Chem. 268*, 3143−9.
18. Loo, T. W., and Clarke, D. M. (1995) Membrane topology of a cysteine-less mutant of human P-glycoprotein, *J. Biol. Chem. 270*, 843−8.
19. Stein, W. D. (1986) *Transport and Diffusion Across Cell Membranes*, Academic Press, New York.
20. Barnett, J. E., Holman, G. D., and Munday, K. A. (1973) Structural requirements for binding to the sugar-transport system of the human erythrocyte, *Biochem. J. 131*, 211−21.
21. Baldwin, S. A., Baldwin, J. M., and Lienhard, G. E. (1982) The monosaccharide transporter of the human erythrocyte. Characterization of an improved preparation, *Biochemistry 21*, 3836−3842.
22. Diamond, D., and Carruthers, A. (1993) Metabolic control of sugar transport by derepression of cell surface glucose transporters: an insulin-independent, recruitment-independent mechanism of regulation, *J. Biol. Chem. 268*, 6437−6444.
23. Hebert, D. N., and Carruthers, A. (1992) Glucose transporter oligomeric structure determines transporter function. Reversible redox-dependent interconversions of tetrameric and dimeric GLUT1, *J. Biol. Chem. 267*, 23829−38.
24. Femino, A. M., Fay, F. S., Fogarty, K., and Singer, R. H. (1998) Visualization of Single RNA Transcripts in Situ, *Science 280*, 585−590.
25. Carruthers, A., Hebert, D. N., Helgerson, A. L., Tefft, R. E., Naderi, S., and Melchior, D. L. (1989) Effects of Calcium, ATP and Membrane lipids on Glucose Transporter Function, *Ann. N.Y. Acad. Sci. 568*, 52−67.
26. Carruthers, A., and Melchior, D. L. (1983) Asymmetric or symmetric? Cytosolic modulation of human erythrocyte hexose transfer, *Biochim. Biophys. Acta 728*, 254−266.
27. Cloherty, E. K., Diamond, D. L., Heard, K. S., and Carruthers, A. (1996) Regulation of GLUT1-mediated sugar transport by an antiport/uniport switch mechanism, *Biochemistry 35*, 13231−13239.
28. Vera, J. C., Reyes, A. M., Velasquez, F. V., Rivas, C. I., Zhang, R. H., Strobel, P., Slebe, J. C., Nunez-Alarcon, J., and Golde, D. W. (2001) Direct inhibition of the hexose transporter GLUT1 by tyrosine kinase inhibitors, *Biochemistry 40*, 777−90.
29. Afzal, I., Cunningham, P., and Naftalin, R. J. (2002) Interactions of ATP, oestradiol, Genistein and the antioestrogens, ICI 182780 (FaslodexTM) and Tamoxifen with the human erythrocyte glucose transporter, GLUT1, *Biochem. J.*, in press.
30. Krupka, R. M., and Devés, R. (1980) Asymmetric binding of steroids to the internal and external sites in the glucose carrier of erythrocytes, *Biochim. Biophys. Acta 598*, 134−144.
31. Weatherman, R. V., Fletterick, R. J., and Scanlan, T. S. (1999) Nuclear-Receptor Ligands and Ligand-Binding Domains, *Annu. Rev. Biochem. 68*, 559−581.
32. Gallivan, J. P., and Dougherty, D. A. (1999) Cation-pi interactions in structural biology. *Proc. Natl. Acad. Sci. U.S.A. 96*, 9459−9464.
33. Sato, M., and Mueckler, M. (1999) A conserved amino acid motif (R-X-G-R-R) in the glut1 glucose transporter is an important determinant of membrane topology [In Process Citation], *J. Biol. Chem. 274*, 24721−5.
34. Schurmann, A., Doege, H., Ohnimus, H., Monser, V., Buchs, A., and Joost, H. G. (1997) Role of conserved arginine and glutamate residues on the cytosolic surface of glucose transporters for transporter function, *Biochemistry 36*, 12897−902.
35. Simpson, I. A., and Cushman, S. W. (1986) Hormonal regulation of mammalian glucose transport, *Annu. Rev. Biochem. 55*, 1059−1089.
36. Cloherty, E. K., Levine, K. B., and Carruthers, A. (2001) The red blood cell glucose transporter presents multiple, nucleotide sensitive sugar exit sites, *Biochemistry 40*, 15549−15561.
37. Wood, R. E., and Morgan, H. E. (1969) Regulation of sugar transport in avian erythrocytes, *J. Biol. Chem. 244*, 1451−1460.
38. Carruthers, A. (1986) ATP regulation of the human red cell sugar transporter, *J. Biol. Chem. 261*, 11028−11037.
39. Jung, C. Y., Carlson, L. M., and Whaley, D. A. (1971) Glucose transport carrier activities in extensively washed human red cell ghosts, *Biochim. Biophys. Acta 241*, 613−627.
40. Harrison, S. A., Buxton, J. M., and Czech, M. P. (1991) Suppressed intrinsic catalytic activity of GLUT1 glucose transporters in insulin-sensitive 3T3-L1 adipocytes, *Proc. Nat. Acad. Sci. U.S.A. 88*, 7839−43.
41. Harrison, S. A., Buxton, J. M., Helgerson, A. L., MacDonald, R. G., Chlapowski, F. J., Carruthers, A., and Czech, M. P. (1990) Insulin action on activity and cell surface disposition of human HepG2 glucose transporters expressed in Chinese hamster ovary cells, *J. Biol. Chem. 265*, 5793−801.

BI0258997